A REGULARIZATION METHOD FOR THE NUMERICAL SOLUTION OF SHALLOW WATER EQUATIONS

T. G. Elizarova* and J.-C. Lengrand†

**Keldysh Institute for Applied Mathematics, Russian Academy of Sciences, Miusskaya sq. 4, 125047 Moscow, Russia*

†CNRS/ICARE, 1C avenue de la recherche scientifique, 45071 Orléans cedex, France

Introduction

Based on a number of hypotheses, the inviscid flow of a liquid can be treated by the so-called *Shallow Water Equations*. This approach has been widely used in the mathematical description of a number of problems [1, 2].

The shallow water equations are closely related to the gasdynamic equations: they can be derived formally from the barotropic approximation of Euler equations. This is why numerical algorithms for solving SWE are often based on numerical methods for Euler equations.

Recently an efficient numerical algorithm for calculations of viscous and inviscid compressible gas flows has been developed. It is based on a special form of regularization in the Navier-Stokes (NS) equations that includes additional dissipative terms. The latter have the form of second-order space derivatives in factor of a small parameter τ. These new equations were called quasi-gasdynamic (QGD) and quasi-hydrodynamic (QHD) equations [3 - 6]. The numerical algorithms based on QGD and QHD equations have shown their efficiency in a number of numerical computations for various problems of fluid dynamics.

In this paper the QGD and QHD additional terms are modified by the same transformation that changes Euler equations into shallow water equations and added to the latter. Regularized Shallow Water (RSW) equations are thus obtained. The corresponding numerical methods are proposed and tested on the problem of hydraulic jump.

Shallow water equations and barotropic approximation of Euler equations

Euler equations in index form write

$$\frac{\partial \rho}{\partial t} + \frac{\partial (\rho u_i)}{\partial x_i} = 0 \tag{1}$$

$$\frac{\partial (\rho u_i)}{\partial t} + \frac{\partial}{\partial x_j}\left(\rho u_j u_i\right) + \frac{\partial p}{\partial x_i} = \rho f_i \tag{2}$$

$$\frac{\partial E}{\partial t} + \frac{\partial}{\partial x_i} u_i (E + p) = \rho u_i f_i \tag{3}$$

The unknown in Eqs (1)-(3) are the gas density $\rho(x_i, t)$, the gas velocity $u_i(x_j, t)$ and the pressure $p(x_i, t)$. The total energy $E(x_i, t)$ per unit-volume is related to these unknown. For a dilute gas with constant specific heats, we have $E = \left(\rho u_i u_i / 2\right) + \left(p / (\gamma - 1)\right)$, where γ is the ratio of specific heats (adiabatic exponent). f_i is an external volume force per unit-mass.

The barotropic approximation consists in reducing the system, assuming that pressure depends only on density as $p = p(\rho)$. Assuming again the gas to be dilute with constant specific heats and its evolution to be adiabatic and reversible (i.e. isentropic), we have

$$dp \,/\, p = \gamma \,(d\rho \,/\, \rho)\,. \tag{4}$$

The shallow water equations for a flow over a plane horizontal bottom write

$$\frac{\partial h}{\partial t} + \frac{\partial (u_i h)}{\partial x_i} = 0 \text{ and } \frac{\partial (hu_i)}{\partial t} + \frac{\partial (hu_j u_i)}{\partial x_j} + \frac{\partial}{\partial x_i}\left[\frac{gh^2}{2}\right] = 0\,, \tag{5}$$

Considering Euler equations in the absence of external volume force, equations (1) and (2) can be formally transformed into equations (5) if the gas density ρ is replaced by h, and the pressure p is replaced by $g\,h^2 \,/\, 2$. This replacement forces a relationship between the variations of ρ and p:

$$dp \,/\, p = 2\,(d\rho \,/\, \rho)\,, \tag{6}$$

consistent with $\gamma = 2$ in Euler equations. The formal change

$$\rho \to h,\; p \to gh^2 \,/\, 2, \gamma \to 2 \tag{7}$$

will be applied to the regularization terms of QGD and QHD equations.

Regularized Shallow Water Equations

A detailed presentation of QGD and QHD equations can be found in [3]. In the absence of external volume forces, both QGD and QHD systems have the general form

$$\frac{\partial \rho}{\partial t} + \frac{\partial j_{mi}}{\partial x_i} = 0\,, \tag{8}$$

$$\frac{\partial (\rho u_i)}{\partial t} + \frac{\partial}{\partial x_j}\left(j_{mj} u_i\right) + \frac{\partial p}{\partial x_i} = \frac{\partial}{\partial x_j}\Pi_{ji} \tag{9}$$

$$\frac{\partial E}{\partial t} + \frac{\partial}{\partial x_i}\, j_{mi}\, \frac{E + p}{\rho} + \frac{\partial}{\partial x_i} q_i = \frac{\partial}{\partial x_j}\Pi_{ji} u_j\,. \tag{10}$$

Here Π_{ij} and q_i are the shear-stress tensor and the heat flux vector, respectively. j_m is a modified mass flux vector, that differs from ρu by a small quantity

$$j_{mi} = \rho(u_i - w_i) \tag{11}$$

with
$$w_i = \frac{\tau}{p}\left(\frac{\partial}{\partial x_j}(\rho u_j u_i) + \frac{\partial}{\partial x_i} p\right) \quad \text{(QGD)} \tag{12}$$

or
$$w_i = \frac{\tau}{p}\left(\rho u_i \frac{\partial u_j}{\partial x_j} + \frac{\partial}{\partial x_i} p\right) \quad \text{(QHD)}\,. \tag{13}$$

Similarly Π is a modified shear-stress tensor, equal to the Navier-Stokes (NS) one plus an additional term.

The additional terms in both QGD and QHD systems involve a small parameter τ that has the dimension of a time. According to the application, τ has a physical meaning (molecular relaxation time in rarefied gas flows, time-averaging parameter in turbulent flows) or can be regarded as purely numerical, the additional terms acting as regularizing terms.

When solving Euler equations for supersonic gas flows, the NS terms Π_{ij} and q_i can be kept as regularizing terms if the coefficients of viscosity μ and thermal conductivity κ are expressed in terms of τ, e.g., $\mu = p\tau$. It was shown that the regularizing additions have a dissipative nature. For stationary flows they have the order of $O(\tau^2)$. A wide range of Euler flow calculations with QGD and QHD models can be found in, e.g., [3] and [5] and citations therein. Recent results are presented in [7] and [8]. The associated algorithms are characterized by the accuracy of the mathematical solution for oscillating flows, the natural adaptation to unstructured space grids and the possibility of efficient implementation on multiprocessor computers. The barotropic approximations of the QGD and QHD equations were studied recently in [9] and [10].

Let us consider the barotropic approximation of Eqs (8)-(10). By applying the formal transformation (7), one obtains two variants of the regularized shallow water equation systems: RSW1 based on the QGD approach and RSW2 based on the QHD approach. We will apply these equations to a hydraulic jump and we restrict here to a 1D flow over a plane horizontal bottom.

RSW1 equations are obtained starting from Eqs 5.51 and 5.52 of [3], applied to a 1D flow:

$$\frac{\partial \rho}{\partial t} + \frac{\partial(\rho u)}{\partial x} = \frac{\partial(\rho w)}{\partial x}, \tag{14}$$

$$\frac{\partial(\rho u)}{\partial t} + \frac{\partial(\rho u^2)}{\partial x} + \frac{\partial p}{\partial x} = \frac{\partial(\rho u w)}{\partial x} + \frac{\partial \Pi}{\partial x}, \text{ with} \tag{15}$$

$$w = \frac{\tau}{\rho} \times \frac{\partial(\rho u^2 + p)}{\partial x}, \ \Pi = \frac{4}{3}\mu \frac{\partial u}{\partial x} + u\tau\left(\rho u \frac{\partial u}{\partial x} + \frac{\partial p}{\partial x}\right) + \tau\left(u\frac{\partial p}{\partial x} + \gamma p \frac{\partial u}{\partial x}\right) . \tag{16}$$

Replacing ρ, p and γ by $h, gh^2/2$ and 2, respectively, one obtains RSW1 equations:

$$\frac{\partial h}{\partial t} + \frac{\partial(uh)}{\partial x} = \frac{\partial(wh)}{\partial x}, \tag{17}$$

$$\frac{\partial(hu)}{\partial t} + \frac{\partial(u^2 h)}{\partial x} + \frac{\partial}{\partial x}\left[\frac{gh^2}{2}\right] = \frac{\partial(huw)}{\partial x} + \frac{\partial \Pi}{\partial x} \tag{18}$$

where $$w = \frac{\tau}{h} \times \frac{\partial(hu^2 + gh^2/2)}{\partial x} \text{ and } \Pi = \frac{4}{3}\mu\frac{\partial u}{\partial x} + \tau g h\left[\left(h + \frac{u^2}{g}\right)\frac{\partial u}{\partial x} + 2u\frac{\partial h}{\partial x}\right] \tag{19}$$

RSW2 equations differ by the regularizing right-hand terms:

$$\frac{\partial h}{\partial t} + \frac{\partial(uh)}{\partial x} = \frac{\partial(wh)}{\partial x}, \tag{20}$$

$$\frac{\partial(hu)}{\partial t} + \frac{\partial(u^2 h)}{\partial x} + \frac{\partial}{\partial x}\left[\frac{gh^2}{2}\right] = 2\frac{\partial(huw)}{\partial x} + \frac{\partial \Pi}{\partial x}, \tag{21}$$

where $$w = \tau\left(u\frac{\partial u}{\partial x} + g\frac{\partial h}{\partial x}\right) \text{ and } \Pi = \frac{4}{3}\mu\frac{\partial u}{\partial x}. \tag{22}$$

The terms $\left[(4/3)\mu\,(\partial u/\partial x)\right]$ in Eqs. (19 and 22) look like a usual viscous term in NS equations. However, the physical viscosity μ is replaced by τp like in QGD equations, i.e. by $\tau g h^2/2$ after the formal transformation. This system (without the NS-like term) has been used in [11] to compute the 1D time evolution of an initial level difference as, i.e. after a dam break.

Numerical test-case: hydraulic jump

Physical problem and analytic solution

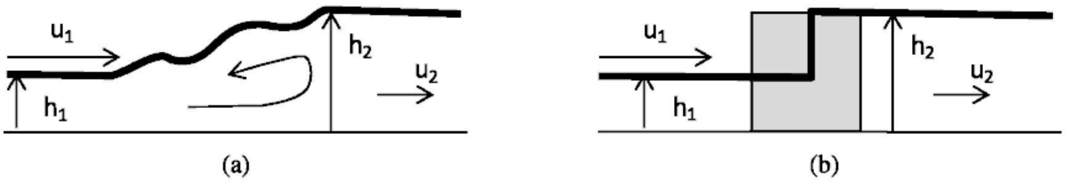

Fig. 1: Hydraulic jump

As a test-case, we treat the 1D flow of an inviscid liquid of density *ρ*, in a uniform gravity field of intensity *g*. The velocity *u* is considered as uniform in a given section. The abscissa *x* refers to the flow direction. The particular problem treated is the hydraulic jump, for which an analytic solution exists [12].

A hydraulic jump is a sudden change in the height *h* and velocity *u* of the flow. Fig. 1a is a schematic view of the physical phenomenon. A 1D approach is not suitable to describe what happens actually. However, a 1D approach is sufficient to express the conservation laws and to relate conditions upstream and downstream of the jump, referred to as (1) and (2), respectively. The problem is simplified as in Fig. 1b. It results from mass conservation that $hu = \text{cste}$, and in particular $h_1 u_1 = h_2 u_2$. We introduce the Froude number, which is the ratio of flow velocity to the velocity of surface waves $c(x,t) = \left(g\,h(x,t)\right)^{1/2}$.

$$\mathrm{Fr} = \frac{u}{(gh)^{1/2}},\ \mathrm{Fr}_1 = \frac{u_1}{(gh_1)^{1/2}} \text{ and } \mathrm{Fr}_2 = \frac{u_2}{(gh_2)^{1/2}}. \tag{23}$$

For a given value of the upstream Froude number, the height ratio across the jump is obtained analytically:

$$\frac{h_2}{h_1} = \frac{1}{2}\left(-1 + \left(1 + 8\,\mathrm{Fr}_1^2\right)^{1/2}\right), \text{ resulting in } h_2 = h_1 \times \frac{h_2}{h_1},\quad u_2 = \frac{h_1\,u_1}{h_2},\ \mathrm{Fr}_2 = \frac{u_2}{\left(g\,h_2\right)^{1/2}}. \tag{24}$$

h_2/h_1 is an increasing function of Fr_1, with the limiting case $h_1 = h_2$ for $\mathrm{Fr}_1 = 1$.

The hydraulic jump equations are perfectly symmetric in (1) and (2). However the second law of thermodynamics requires that the hydraulic energy (specific head) does not increase. Therefore $\left(h_1 + u_1^2/2\right) - \left(h_2 + u_2^2/2\right)$ must be not negative. This requires $\mathrm{Fr}_1 \geq 1$ (torrential regime) and therefore $h_2 \geq h_1, u_2 \leq u_1, \mathrm{Fr}_2 \leq 1$ (fluvial regime). A hydraulic jump is equivalent to a normal shock in a 1D gas flow that makes the flow switch from supersonic (Mach number >1) to subsonic (Mach number <1). The hydraulic jump is a rather severe test-case, due to the discontinuity.

Numerical algorithm

As was done for QGD and QHD equations, the RSW1 and RSW2 equations were solved by an explicit finite-volume approach, using a central finite-difference approximation for all terms, including the convective ones. The regularizing terms are favorable to the stability of the solution. They act as artificial dissipation and depend on a single parameter τ which was taken *locally* as

$$\tau(x,t) = \alpha\ \Delta x / c(x,t)\,, \tag{25}$$

where Δx is the computational grid step. The value of α must ensure stability, while keeping the results close to the exact solution.

The time step was taken from the Courant stability condition

$$\Delta t = \beta \min(\Delta x / c(x,t)) = \beta \min(\Delta x / (g\ h)^{1/2})\,, \tag{26}$$

where the minimum is calculated over all grid points at a given time. The constant β has to be adjusted to ensure stability. Δt should be readjusted at each time step and should become constant when convergence is approached. However for the present problem, the maximal value of h at convergence is $h = h_2$. Therefore, we do not readjust it during the calculation and we take

$$\Delta t = \beta \times (\Delta x / (g\ h_2)^{1/2})\,. \tag{27}$$

A parametric study was carried out to determine the domain of convergence of the algorithm in terms of α and β for different values of Fr_1, and to check the correctness of the numerical solution, compared with the analytical one, schematized in Fig.1b.

The acceleration of gravity was taken equal to 9.81 $\mathrm{m.s^{-2}}$. h_1 was taken arbitrarily equal to 1 m. The values of u_1, u_2, h_2 were calculated from Eq.24 and used to prescribe the boundary conditions. The initial conditions were characterized by a smooth variation of h from h_1 at input to h_2 at output and the corresponding velocity $u = (h_1 u_1)/h$.

Unless otherwise specified, the computational domain had a length L = 100m and was divided into N = 500 intervals of size $\Delta x = 0.2\,\mathrm{m}$. The calculations were stopped at a predefined maximal physical time. Convergence was monitored by recording the adimensional residues

$$\mathrm{res}_{\mathrm{avg}} = \frac{1}{N-1}\sum_{i=1}^{N-1}\left|\frac{u_i^{j+1} - u_i^j}{u_i^j}\right|\ . \tag{28}$$

The calculations were carried out on a personal computer, using double precision. The CPU time depends directly on the value of β.

The length of the computational domain was much larger than the jump thickness. Physically, the position of the jump in the computational domain is undetermined. Therefore, the profiles can be arbitrarily translated along the *x*-axis. Their exact position is not significant. However, in the present figures, their position is indicated as obtained by the calculation. When the calculations converged, the final residues were very small, probably governed by the computer precision, i.e. the final state was perfectly steady.

Results for RSW1

Computations were carried out for the first variant of RSW equations (RSW1). Hydraulic jumps were successfully calculated with

$$\mathrm{Fr}_1 = 1.1,\ h_1 = 1\,\mathrm{m},\ u_1 = 3.445\,\mathrm{m/s},\ h_2 = 1.134\,\mathrm{m},\ u_2 = 3.038\,\mathrm{m/s}$$

$$\mathrm{Fr}_1 = 2,\ h_1 = 1\,\mathrm{m},\ u_1 = 6.264\,\mathrm{m/s},\ h_2 = 2.372\,\mathrm{m},\ u_2 = 2.641\,\mathrm{m/s}$$

$$\mathrm{Fr}_1 = 5,\ h_1 = 1\,\mathrm{m},\ u_1 = 15.66\,\mathrm{m/s},\ h_2 = 6.589\,\mathrm{m},\ u_2 = 2.377\,\mathrm{m/s}$$

$$\mathrm{Fr}_1 = 10,\ h_1 = 1\,\mathrm{m},\ u_1 = 31.32\,\mathrm{m/s},\ h_2 = 13.65\,\mathrm{m},\ u_2 = 2.294\,\mathrm{m/s}\ .$$

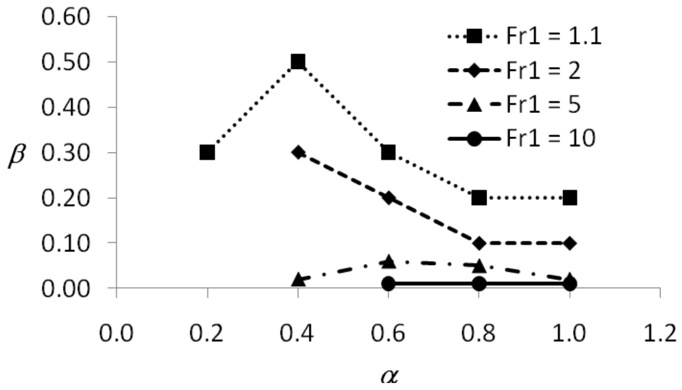

Fig.2: Maximal admissible value of β as a function of α and Fr_1 (RSW1)

For each test-case, different values of α were used. For a given α, different runs with increasing values of β were computed until divergence. The highest admissible value of β is plotted in Fig. 2 as a function of α and Fr_1. It could be expected that increasing α would allow increasing β and reducing computational time. This is not true for $\alpha > 0.5$-0.6.

Only the results obtained for Fr1 =2 and Fr1 = 10 will be discussed here.

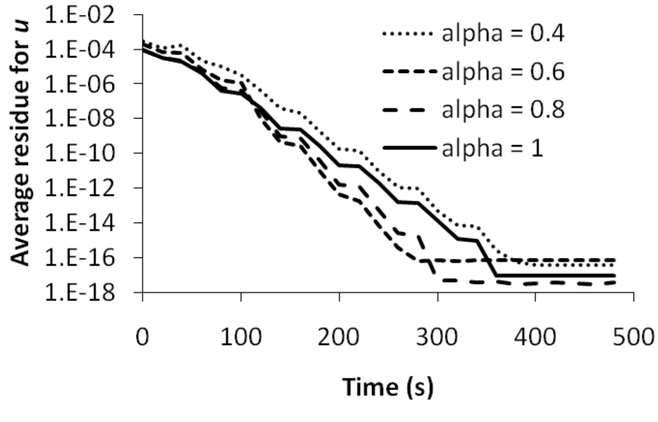

Fig.3: Convergence history for Fr_1 = 2 (RSW1)

The convergence history and the spatial distribution of depth h for Fr_1 = 2 are plotted in Figs.3 and 4, respectively. All grid points in the vicinity of the jump have been plotted. The jump is very stiff (1-2 grid steps from the minimal to the maximal values) and accompanied by oscillations that decrease with increasing α.

The convergence history and the spatial distribution of depth h for Fr_1 = 10 are plotted in Fig.5 and 6, respectively. The choice of α does not affect much the convergence rate, nor the stiffness of the jump. The jump is still very stiff (1-2 grid steps). However, it is clear that small values of α lead to unacceptable oscillations. The profile decreases strongly ahead of the physical jump: h is as low as 0.35 m for $\mathrm{Fr}_1 = 10$ and $\alpha = 0.6$.

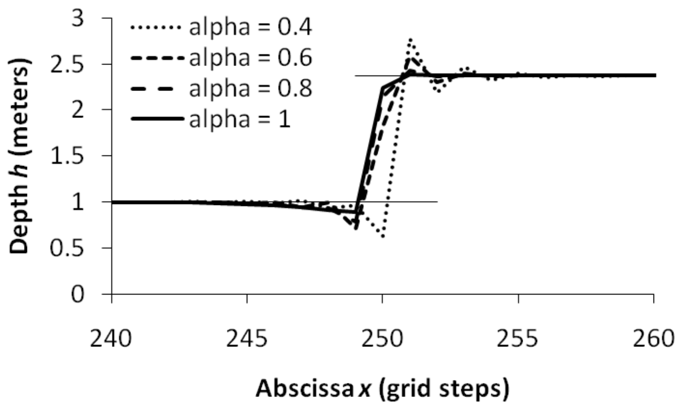

Fig.4: Distribution of depth for $\mathrm{Fr}_1 = 2$ (RSW1)

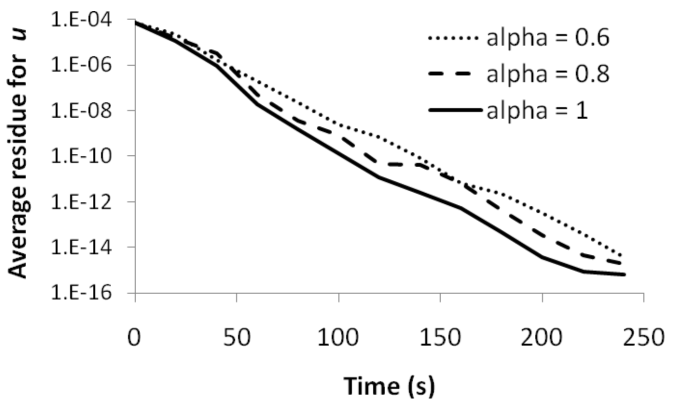

Fig.5: Convergence history for $\mathrm{Fr}_1 = 10$ (RSW1)

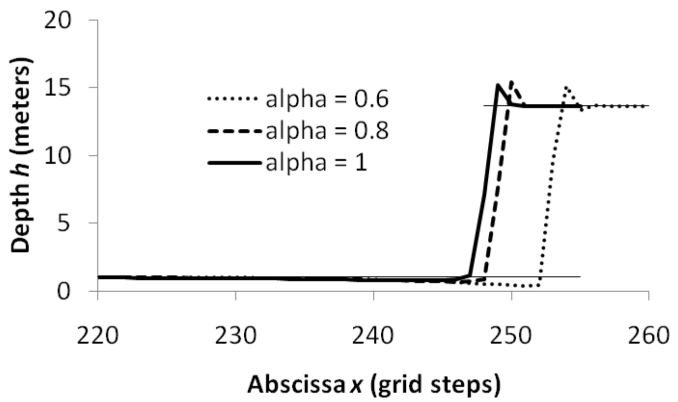

Fig.6: Distribution of depth for $\mathrm{Fr}_1 = 10$ (RSW1)

The initial height profile was a *smooth* variation between h_1 and h_2. Using either a linear or a sinusoidal initial profile resulted in the same convergence rate and indistinguishable final profiles.

As explained above, the NS-like terms can be kept as regularizing terms, as was done in the calculations presented above. Because the regularization has a somewhat arbitrary character, one of the runs was repeated with the NS-like terms removed. The term $\left[(4/3)\mu\,(\partial u/\partial x)\right]$ was removed from Π in Eqs.(16) and (19). The convergence is much slower. However, the final profiles are very similar (Figs.7 and 8) if we remember that the profiles can be translated arbitrarily along the *x*-axis.

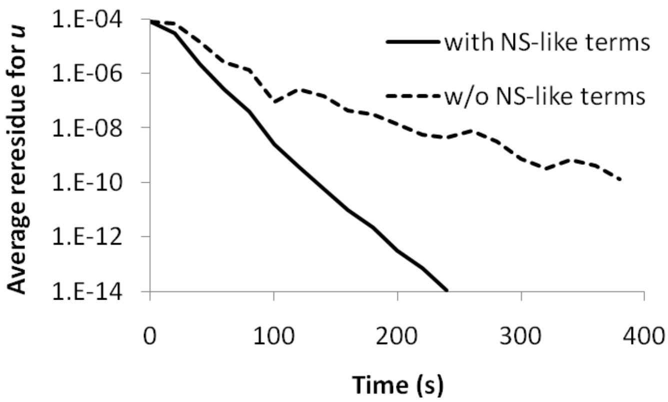

Fig.7: Convergence history for Fr_1 = 10, α = 0.6 (RSW1, influence of NS-like regularizing terms)

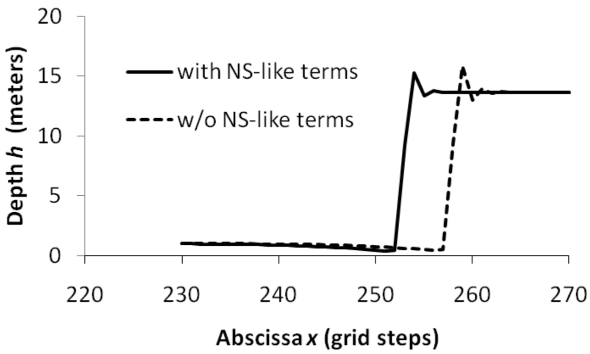

Fig.8: Distribution of depth for Fr_1 = 10, α = 0.6 (RSW1, influence of NS-like regularizing terms)

Results for RSW2

A similar approach was applied to the second variant of RSW equations (RSW2). For a given Froude number and a given α, different runs with increasing values of β were computed until divergence. The highest acceptable value of β was retained.

The first case considered was characterized by

$$\mathrm{Fr}_1 = 1.1,\ h_1 = 1\,\mathrm{m},\ u_1 = 3.445\,\mathrm{m/s},\ h_2 = 1.134\,\mathrm{m},\ u_2 = 3.038\,\mathrm{m/s}\,.$$

The convergence history and the spatial distribution of depth h are plotted in Figs.9 and10, respectively. Increasing α from 0.05 to 0.5 reduces the oscillations of the solution and simultaneously thickens the jump. This increases the stability of the equation system and allows increasing β and reducing the computing time. However, as already observed for RSW1, increasing α beyond 0.5 does not allow a further increase of β.

Using a grid step twice larger than indicated before, the thickness of the jump was found identical in terms of grid steps.

The length of the computational domain was much larger than the jump thickness and did not affect the final profile, when changed from 100 to 200 m.

A similar set of calculations was carried out for

$$\mathrm{Fr}_1 = 2,\ h_1 = 1\,\mathrm{m},\ u_1 = 6.264\,\mathrm{m/s},\ h_2 = 2.372\,\mathrm{m},\ u_2 = 2.641\,\mathrm{m/s}\,.$$

A value of α at least equal to 0.5 was required for convergence.

Finally, a hydraulic jump with

$$\mathrm{Fr}_1 = 2.5,\ h_1 = 1\,\mathrm{m},\ u_1 = 7.830\,\mathrm{m/s},\ h_2 = 3.071\,\mathrm{m},\ u_2 = 2.550\,\mathrm{m/s}$$

was calculated. Only one set of parameters $(\alpha = 1, \beta = 0.05)$ resulted in a converged result.

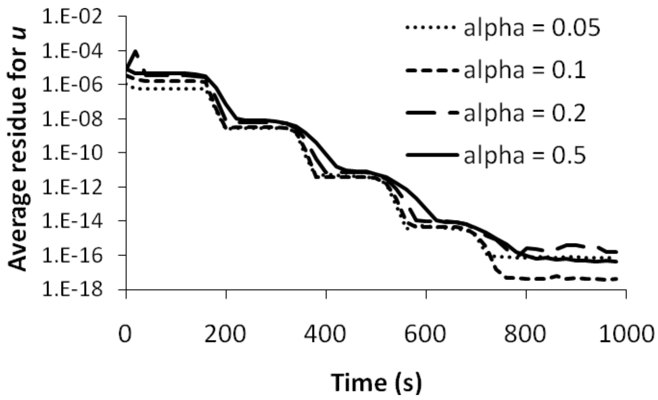

Fig.9: Convergence history and distribution of depth for Fr_1 = 1.1(RSW2)

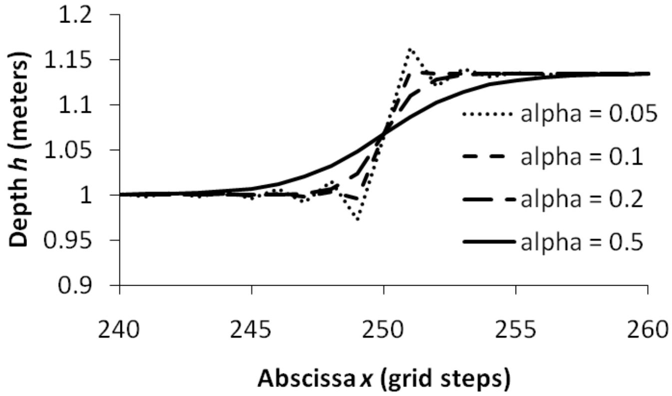

Fig.10: Convergence history and distribution of depth for Fr_1 = 1.1 (RSW2)

For Fr1 = 3, no combination of parameters (α, β) could be found to ensure convergence.

The maximal admissible value of β to be used when computing a hydraulic jump with the RSW2 equations is plotted in Fig.11 as a function of α and Fr_1.

For the present test-case, no converged result could be obtained with the NS-like terms removed.

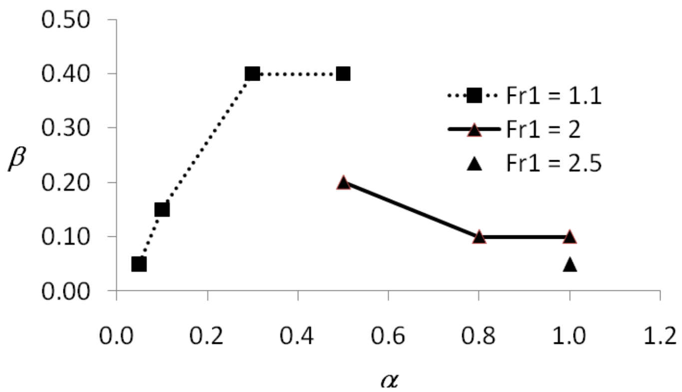

Fig.11: Maximal admissible value of β as a function of α and Fr_1 (RSW1)

Conclusion

The shallow water equations have been completed by regularization terms derived from additional terms contained in the *Quasi-GasDynamic* (QGD) and *Quasi-HydroDynamic* (QHD) equations. Although developed for gases, these terms could be applied to a liquid flow by considering the formal analogy between Euler equations and shallow water equations. Two variants of the resulting *Regularized Shallow Water* (RSW) equations were presented: RSW1 based on QGD terms and RSW2 based on QHD terms.

The regularizing terms involve an adjustable parameter α. Increasing α increases the stability of the system and allows the RSW equations being solved with a simple numerical algorithm, rather than by the high-order numerical schemes that are frequently used.

RSW equations have been applied to a test-case consisting in a hydraulic jump, characterized by its upstream Froude number Fr_1. A parametric study has been carried out on this test-case. The analytic solution served as a reference. The numerical solution could reproduce the discontinuity satisfactorily, with a jump thickness of 1-2 grid steps.

The computational time step is governed by the Courant parameter β. The maximum admissible value of β depends on Fr_1 and α. Although the additional terms improve the stability of the system, increasing α beyond approx. 0.5 does not allow a further increase in the time step.

Hydraulic jumps with Fr_1 as high as 10 could be calculated efficiently with RSW1 equations. The limits of the acceptable (α, β) domain have been indicated.

RSW2 equations have a smaller domain of application. No acceptable combination of (α, β) could be found for upstream Froude numbers larger than 2.5.

The additional terms may include or not Navier-Stokes-like viscosity terms. The presence of these terms accelerates convergence (RSW1) or is even required for convergence (RSW2).

The system converges fast with decreasing the mesh step. RSW methods may be efficiently generalized for unstructured triangular grids and may be efficiently implemented in modern multiprocessor and multinuclear calculation modules.

They appear as promising tools for the simulation of flows in real natural conditions.

ACKNOWLEDGMENT

This work has been supported by the *Fund for Fundamental Researches* of the RAS under reference 10-01-00136.

REFERENCES

1. **Stoker J.J.** Water waves, The Mathematical Theory with Applications, Interscience, New York , 1957.
2. **Landau L.D., Lifshitz E.M.** Hydrodynamics, Nauka, Moscow, 1986 (in Russian).
3. **Elizarova T.G.** Quasi-Gas Dynamic equations, Springer, 2009.
4. **Elizarova T.G., Khokhlov A.A, Sheretov Yu.V.** Quasi-gasdynamic numerical algorithm for gas flow simulations, Intern. J. for Numer. Meth. in Fluids 2008. Vol. 56. P. 1209 – 1215.
5. **Sheretov Yu. V.** Dynamics of continuum media for spatial-time averaging, Izevsk, Moscow, 2009 (in Russian).
6. **Chetverushkin B.N.** Kinetic Schemes and Quasi-Gasdynamic System of Equations, MAKS, Moscow, 2004.
7. **Elizarova T.G. Shil'nikov E.V.** Capabilities of a Quasi-Gasdynamic Algorithm as Applied to Inviscid Gas Flow Simulations, Computational Mathematics and Mathematical Physics 2009. Vol. 49, P. 549 – 566.
8. **Elizarova T.G. Shil'nikov E.V.** Numerical Analysis of a Quasi-Gasdynamic Algorithm as Applied to the Euler Equations, Computational Mathematics and Mathematical Physics 2009. Vol. 49, P. 1869 – 1884.
9. **Zlotnik A.A, Chetverushkin B.N.** Parabolicity of the Quasi-Gasdynamic System of Equations, its Hyperbolic Second-Order Modification, and the Stability of Small Perturbations for them, Computational Mathematics and Mathematical Physics 2008. Vol. 48, P. 420 – 446.
10. **Zlotnik A.A.**, Energy Equalities and Estimates for Barotropic Quasi-Gasdynamic and Quasi-Hydrodynamic Systems of Equations, Computational Mathematics and Mathematical Physics 2010. Vol. 50, P. 310 – 321.
11. **Elizarova T.G., Afanasieva M.V.** Regularized shallow water equations, Moscow University Physics Bulletin 2010. Vol. 65, P. 13 - 16, Allerton Press, Inc.
12. **Elizarova T.G., Lengrand J.-C.** A regularization method for the numerical solution of Shallow Water Equations, 5th European Conference on Computational Fluid Dynamics, ECCOMAS CFD2010., Lisbon, Portugal, June 14-17, 2010, CD-ROM Proceedings, paper 01621.